JACS
JOURNAL OF THE AMERICAN CHEMICAL SOCIETY

COMMUNICATION

pubs.acs.org/JACS

Synthesis of Ultrathin FePtPd Nanowires and Their Use as Catalysts for Methanol Oxidation Reaction

Shaojun Guo, Sen Zhang, Xiaolian Sun, and Shouheng Sun*

Department of Chemistry, Brown University, Providence, Rhode Island 02912, United States

Supporting Information

ABSTRACT: We report a facile synthesis of ultrathin (2.5 nm) trimetallic FePtPd alloy nanowires (NWs) with tunable compositions and controlled length (<100 nm). The NWs were made by thermal decomposition of $Fe(CO)_5$ and sequential reduction of $Pt(acac)_2$ (acac = acetylacetonate) and $Pd(acac)_2$ at temperatures from 160 to 240 °C. These FePtPd NWs showed composition-dependent catalytic activity and stability for methanol oxidation reaction. Among FePtPd and FePt NWs as well as Pd, Pt, and PtPd nanoparticles (NPs) studied in 0.2 M methanol and 0.1 M $HClO_4$ solution, the $Fe_{28}Pt_{38}Pd_{34}$ NWs showed the highest activity, with their mass current density reaching 488.7 mA/mg Pt and peak potential for methanol oxidation decreasing to 0.614 V from 0.665 V (Pt NP catalyst). The NW catalysts were also more stable than the NP catalysts, with the $Fe_{28}Pt_{38}Pd_{34}$ NWs retaining the highest mass current density (98.1 mA/mg Pt) after a 2 h current−time test at 0.4 V. These trimetallic NWs are a promising new class of catalyst for methanol oxidation reaction and for direct methanol fuel cell applications.

Synthesis of ultrathin (<10 nm) metallic nanowires (NWs) has attracted considerable interest due to the unique magnetic, electronic, and catalytic properties induced by the confined one-dimensional nanostructure.[1−6] FePt alloy NWs with a wire diameter of ∼2 nm are made by thermal decomposition of $Fe(CO)_5$ and reduction of $Pt(acac)_2$ (acac = acetylacetonate) in oleylamine (OAm).[2] These FePt NWs can be assembled and converted into ferromagnetic FePt arrays with preferred magnetic alignment. Single-crystalline Au NWs with diameters <10 nm are synthesized by the reduction of $HAuCl_4$ using OAm or other reducing agents,[3] and the 9 nm Au NWs show good electron conductivity with the breakdown current density reaching 3.5×10^{12} A/m^2.[3a] Recently, ultrathin NWs were also found to be robust catalysts for various chemical reactions. For example, Pt NWs, made by chemical reduction of H_2PtCl_6 using formic acid as reductant, and core/shell-type Pd/Pt NWs, prepared by Cu underpotential deposition on Pd NWs and followed by galvanic displacement of Cu, are more efficient in catalyzing oxygen reduction reaction than other forms of the Pt catalysts.[4,5] PtM (M = Pd, Ru, Au, Fe, Co) alloy NWs and their networks are made available via a soft template formed by cetyltrimethylammonium bromide in a two-phase water−chloroform system for hydrogenation and composition-dependent catalytic studies.[6]

Herein, we report a one-pot synthesis of ultrathin trimetallic FePtPd alloy NWs with controllable length, diameter, and compositions as efficient catalysts for methanol oxidation reaction (MOR). We recently developed a facile synthesis of 2 nm wide FePt NWs via decomposition of $Fe(CO)_5$ and reduction of $Pt(acac)_2$ in the presence of OAm or a mixture of OAm and 1-octadecene (ODE).[2] The composition of FePt NWs was tuned by the molar ratio of $Fe(CO)_5/Pt(acac)_2$, and their length was controlled by the volume ratio of OAm/ODE. By adding sodium oleate and adjusting the addition sequence of precursors, we succeeded in making composition-tunable FePtPd NWs with controlled diameter (2.5 nm) and length (<100 nm). We found that these FePtPd NWs had a strong interaction with carbon supports and were less vulnerable than conventional nanoparticles (NPs) to dissolution, Ostwald ripening, and aggregation in strongly acidic electrocatalytic conditions. They showed high activity and good stability for MOR in 0.1 M $HClO_4$ solution, and their activity/stability were composition-dependent, with $Fe_{28}Pt_{38}Pd_{34}$ NWs having the lowest methanol oxidation peak potential and being the most efficient catalyst for MOR.

The FePtPd alloy NWs were synthesized by thermal decomposition of $Fe(CO)_5$ and controlled reduction of $Pt(acac)_2$ and $Pd(acac)_2$ (see the Supporting Information (SI)). Briefly, 0.3 g of sodium oleate was dissolved in 12 mL of ODE by heating the mixture to 180 °C. The solution was cooled to 60 °C. Next, 0.1 g (0.25 mmol) of $Pt(acac)_2$ dissolved in 8 mL of OAm was added, and the solution was reheated to 120 °C. After the introduction of $Fe(CO)_5$ (0.07 mL, 0.532 mmol), the solution was heated to 160 °C. Then, 75 mg (0.25 mmol) of $Pd(acac)_2$ dissolved in 2 mL of OAm + ODE (volume ratio of 2:3) was added, and the solution was further heated to 240 °C at a heating rate of 4−5 °C/min and kept at 240 °C for 30 min before it was cooled. The product was separated and redispersed in hexane.

Inductively coupled plasma-atomic emission spectroscopy (ICP-AES) was used to characterize the composition of the as-prepared NWs. In the above synthesis, $Fe_{28}Pt_{38}Pd_{34}$ NWs were obtained. If no $Pd(acac)_2$ was added, $Fe_{68}Pt_{32}$ NWs were separated. With a fixed amount of $Fe(CO)_5$, the composition of FePtPd NWs was tuned by controlling the molar ratio of $Pt(acac)_2$ and $Pd(acac)_2$. Under the same reaction conditions as in the synthesis of $Fe_{28}Pt_{38}Pd_{34}$ NWs, 50 mg (0.167 mmol) and 25 mg (0.0835 mmol) of $Pd(acac)_2$ resulted in $Fe_{43}Pt_{34}Pd_{23}$ and $Fe_{58}Pt_{32}Pd_{10}$ NWs, respectively.

The NWs were characterized by transmission electron microscopy (TEM), high-resolution TEM (HRTEM), and X-ray

Received: August 6, 2011
Published: September 06, 2011

ACS Publications © 2011 American Chemical Society

dx.doi.org/10.1021/ja207308b | J. Am. Chem. Soc. 2011, 133, 15354–15357

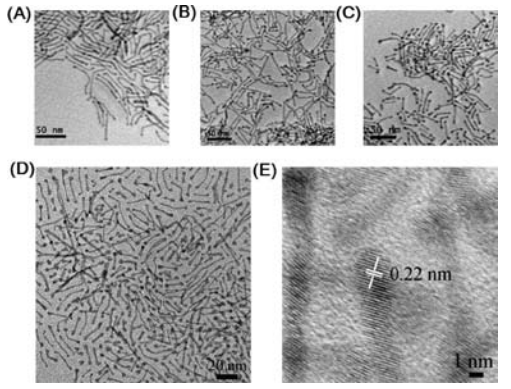

Figure 1. TEM (A–D) and HRTEM (E) images of $Fe_{68}Pt_{32}$ (A), $Fe_{58}Pt_{32}$ Pd_{10} (B), $Fe_{43}Pt_{34}Pd_{23}$ (C), and $Fe_{28}Pt_{38}Pd_{34}$ NWs (D,E).

diffraction (XRD). Figure 1A–D shows typical TEM images of the as-prepared $Fe_{68}Pt_{32}$, $Fe_{58}Pt_{32}Pd_{10}$, $Fe_{43}Pt_{34}Pd_{23}$, and $Fe_{28}Pt_{38}Pd_{34}$ NWs. These NWs have a diameter of 2.5 ± 0.3 nm. The HRTEM image of a single NW, as shown in Figure 1E, reveals that the spacing of the adjacent fringes along the wire growth direction is 0.22 nm, corresponding to the {111} interplanar distance of face-centered cubic FePtPd. Another feature of these NWs is that each NW has two larger tips on both ends. This is similar to what is seen in FePt NWs, indicating that the growth of Pd over FePt NWs does not change the overall NW morphology and the large tips are formed by the preferential growth of FePt and Pd at the end due to the low packing density of the surfactant at the tip.[2] XRD patterns of FePt and FePtPd NWs with different compositions and PtPd NPs are shown in Figure S1. Compared with that of PtPd alloy NPs, the diffraction peaks of FePtPd and FePt NWs shift to larger diffraction angles, indicating reduction of the crystal lattice induced by alloying Fe with Pt or PtPd structure. FePtPd and FePt NWs have very similar diffraction patterns due to the close lattice spacing between Pd- and Pt-based structures. The broadened diffraction peaks from NWs reveal the small dimension of the crystal domains, further proving the ultrathin character of these NWs.[7]

The growth of FePtPd NWs was closely monitored during the synthesis. Before $Pd(acac)_2$ was added to the reaction mixture, the FePt product was separated from the solution heated at 160 °C and characterized by TEM (Figure S2A). We can see that thin FePt NWs are already present. Furthermore, the molar ratio of Fe/Pt between two precursors is carried over to the final FePt product. This implies that the current synthesis gives a high-yield formation of FePt NWs. With the addition of $Pd(acac)_2$ in the reaction mixture containing FePt NWs, the percentage of Fe in the final product is decreased, and its change in atomic ratio is correlated with the amount of $Pd(acac)_2$ added. For example, in the synthesis of $Fe_{28}Pt_{38}Pd_{34}$ NWs, if the original molar ratio of the precursors is carried over to the final FePtPd, then we would expect the formation of $Fe_{52}Pt_{24}Pd_{24}$ NWs. The actual formation of $Fe_{28}Pt_{38}Pd_{34}$ NWs seems to indicate that, upon the addition of $Pd(acac)_2$, Pd(II) is reduced by Fe in FePt NWs via galvanic replacement reaction ($Fe + Pd^{2+} \rightarrow Fe^{2+} + Pd$), forming Pd-coated FePt NWs. With extended heating at 240 °C for 30 min, Pd diffuses into FePt NWs and forms trimetallic $Fe_{28}Pt_{38}Pd_{34}$ alloy NWs. This alloy formation induced by galvanic replacement is similar to what has been observed in the growth of AuAg alloy nanocages.[8] We should note that the sequential addition of

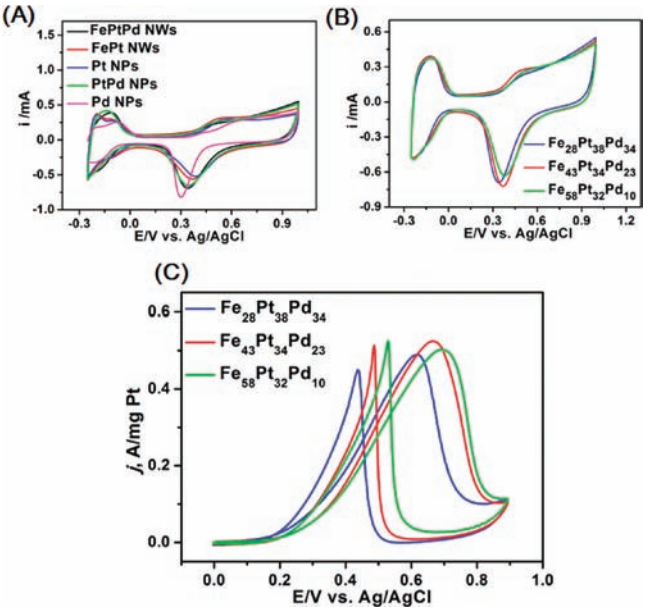

Figure 2. CVs of (A) $Fe_{28}Pt_{38}Pd_{34}$ NWs, FePt NWs, Pt NPs, Pd NPs and PtPd NPs and (B) FePtPd NWs with different compositions in N_2-saturated 0.1 M $HClO_4$ solution at a scan rate of 50 mV/s. (C) CVs of MOR catalyzed by FePtPd NWs with different compositions in N_2-saturated 0.1 M $HClO_4$ and 0.2 M methanol solution at a scan rate of 50 mV/s.

$Pt(acac)_2$ and $Pd(acac)_2$ as described above is essential for the formation of alloy NWs. When $Pt(acac)_2$ and $Pd(acac)_2$ were added together before introducing $Fe(CO)_5$ at 120 °C, only irregular NPs were formed (Figure S2B).

In addition to FePt and FePtPd NWs, ~3 nm Pt NPs,[9] ~5 nm Pd NPs,[10] and ~4 nm $Pt_{48}Pd_{52}$ alloy NPs[11] were made by previous methods. Figure S3 shows the TEM images of these NPs. They were used as controls to compare with the trimetallic FePtPd NWs in electrochemical and electrocatalytic studies.

The as-synthesized FePtPd NWs were further characterized by their electrochemical properties. To perform the tests, the NWs or NPs were first deposited on a carbon support (Kejen EC 300J) via sonication of equal amounts of two constituents in a mixture of hexane and acetone and then washed with acetic acid (99%) at 70 °C to remove the surfactant.[10] During this acid wash, part of Fe in FePtPd NWs was etched away, as confirmed by the composition change from $Fe_{58}Pt_{32}Pd_{10}$, $Fe_{43}Pt_{34}Pd_{23}$, and $Fe_{28}Pt_{38}Pd_{34}$ NWs to $Fe_{49}Pt_{39}Pd_{12}$, $Fe_{36}Pt_{37}Pd_{27}$, and $Fe_{24}Pt_{34}Pd_{32}$ NWs, respectively. The treated NWs/C or NPs/C were redispersed in deionized water + isopropanol (v:v 4:1) to reach a concentration of 2 mg/mL. Nafion at a concentration of 0.025% was also added into the dispersion. Next, 20 μL of this dispersion was deposited on the surface of glassy carbon electrode, and the NWs (or NPs) were fixed onto the electrode by Nafion once the solvent was evaporated. Figure 2A summarizes the typical cyclic votammograms (CVs) of $Fe_{28}Pt_{38}Pd_{34}$ NWs, $Fe_{68}Pt_{32}$ NWs, Pt NPs, Pd NPs and PtPd NPs in N_2-saturated 0.1 M $HClO_4$. In the positive scan, metals/alloys are oxidized at 0.51–0.65 V. In the negative scan, the oxidized metals/alloys are reduced at 0.3–0.39 V. The reduction peak potential of the FePtPd NWs is similar to that of PdPt, but is between those of Pt, FePt and Pd. The composition effects of FePtPd NWs on oxidation and reduction behaviors of the FePtPd NWs were also studied (Figure 2B). With the increase of Pd

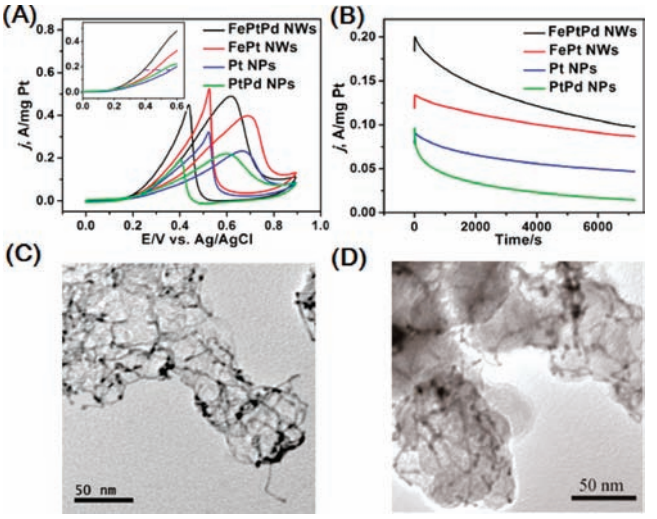

Figure 3. CVs (A), linear sweep voltammetry (inset), and $i-t$ curves (B) of MOR catalyzed by $Fe_{28}Pt_{38}Pd_{34}$ NWs, FePt NWs, Pt NPs, and PtPd NPs in 0.1 M $HClO_4$ + 0.2 M methanol solution. The CVs were obtained at a scan rate of 50 mV/s, and the $i-t$ curves were collected at a constant potential of 0.4 V. TEM images of the $Fe_{28}Pt_{38}Pd_{34}$ NWs/C before (C) and after (D) 2 h $i-t$ test.

concentration in FePtPd structure, the reduction peak potential of FePtPd NWs is negatively shifted. From Figure 2A,B, we can conclude that FePtPd NWs are formed as an alloy, not as a core/shell, structure.

The FePtPd NWs are electrocatalytically active for MOR. The electro-oxidation curves of these NWs in 0.1 M $HClO_4$ and 0.2 M methanol solution are shown in Figure 2C. Among three kinds of FePtPd NWs investigated, $Fe_{28}Pt_{38}Pd_{34}$ NWs have the highest activity by displaying less positive oxidation peak potential at 0.614 V and high mass current density at 488.7 mA/mg Pt. The catalytic performance of $Fe_{28}Pt_{38}Pd_{34}$ NWs was further compared with Pt, PtPd and FePt catalysts (the Pd catalyst was not active for MOR, see Figure S4). Figure 3A shows the CVs of MOR catalyzed by $Fe_{28}Pt_{38}Pd_{34}$ NWs, $Fe_{68}Pt_{32}$ NWs, 3 nm Pt NPs and 4 nm $Pt_{48}Pd_{52}$ alloy NPs in a solution containing 0.1 M $HClO_4$ and 0.2 M methanol. We can see that the $Fe_{28}Pt_{38}Pd_{34}$ NWs have a significant increase in peak current density and a negative potential shift in methanol oxidation over Pt, PtPd and FePt catalysts. The $Fe_{28}Pt_{38}Pd_{34}$ NWs have also the lowest potential for MOR at the same oxidation current density (the inset of Figure 3A). These indicate that $Fe_{28}Pt_{38}Pd_{34}$ NWs have much enhanced catalytic activity for MOR.

Chronoamperometry, a useful method for evaluation of electrocatalyst stability in fuel cells,[12] was employed to investigate the electrochemical activity and stability of different catalysts. Figure S5 in the SI and Figure 3B are typical current (i)−time (t) test results on various catalysts. We can see that the FePtPd NWs have the highest activity among all catalysts studied both before and after the 2 h $i-t$ test. Figure 3B also shows that the Pd-containing catalysts have a faster decay rate than the non-Pd catalysts. These indicate that Pd in the alloy structure is not very stable in acidic MOR conditions and can be etched away readily. Catalyst morphology change during the $i-t$ test was monitored by TEM, as shown in Figure 3C,D and SI Figures S6 and S7. The FePtPd and FePt NWs have no noticeable morphology change before and after the test, whereas Pt NPs show signs of aggregation. This enhanced stability of NWs vs NPs is likely caused by stronger NW interactions with carbon support and/or better NW structure stability,[4,13] which makes the NWs less subject to dissolution, Ostwald ripening, and aggregation than NPs in acidic MOR conditions.

In summary, we have developed a facile synthesis of ultrathin trimetallic FePtPd alloy NWs by thermal decomposition of $Fe(CO)_5$ and sequential reduction of $Pt(acac)_2$ and $Pd(acac)_2$. The key to the successful synthesis is that FePt NWs should be made first and then Pd allowed to deposit on the FePt NWs via a galvanic replacement of Fe with Pd followed by a high-temperature (240 °C) reaction. The FePtPd NWs have diameter ~2.5 nm and length <100 nm. More importantly, due to the molar ratio carryover from the precursors to the product, the compositions of these trimentallic NWs are readily tuned. These FePtPd NWs show composition-dependent MOR activity and stability, and $Fe_{28}Pt_{38}Pd_{34}$ NWs are the most efficient MOR catalysts with their mass current density reaching 488.7 mA/mg Pt and oxidation peak potential decreased to 0.614 V from 0.665 V (Pt NP catalyst). The reported synthesis should offer a general approach to trimetallic NWs as a promising new class of catalyst for direct methanol fuel cells and other advanced catalytic applications.

■ ASSOCIATED CONTENT

Ⓢ Supporting Information. Detailed synthesis of trimetallic NWs and additional characterization data. This material is available free of charge via the Internet at http://pubs.acs.org.

■ AUTHOR INFORMATION

Corresponding Author
ssun@brown.edu

■ ACKNOWLEDGMENT

The work was supported in part by ExxonMobil Research and Engineering Co.

■ REFERENCES

(1) (a) Cademartiri, L.; Ozin, G. A. *Adv. Mater.* **2009**, *21*, 1013–1020. (b) Wang, C.; Sun, S. *Chem. Asian J.* **2009**, *4*, 1028–1034.
(2) Wang, C.; Hou, Y.; Kim, J.; Sun, S. *Angew. Chem., Int. Ed.* **2007**, *46*, 6333–6335.
(3) (a) Wang, C.; Hu, Y.; Lieber, C. M.; Sun, S. *J. Am. Chem. Soc.* **2008**, *130*, 8902–8903. (b) Lu, X.; Yavuz, M. S.; Tuan, H.-Y.; Korgel, B. A.; Xia, Y. *J. Am. Chem. Soc.* **2008**, *130*, 8900. (c) Huo, Z.; Tsung, C.-K.; Huang, W.; Zhang, X.; Yang, P. *Nano Lett.* **2008**, *8*, 2041–2044. (d) Xu, J.; Wang, H.; Liu, C.; Yang, Y.; Chen, T.; Wang, Y.; Wang, F.; Liu, X.; Xing, B.; Chen, H. *J. Am. Chem. Soc.* **2010**, *132*, 11920–11922. (e) Pazos-Prez, N.; Baranov, D.; Irsen, S.; Hilgendorff, M.; Liz-Marzn, L. M.; Giersig, M. *Langmuir* **2008**, *24*, 9855–9860. (f) Feng, H.; Yang, Y.; You, Y.; Li, G.; Guo, J.; Yu, T.; Shen, Z.; Wu, T.; Xing, B. *Chem. Commun.* **2009**, *45*, 1984–1986.
(4) Sun, S.; Zhang, G.; Geng, D.; Chen, Y.; Li, R.; Cai, M.; Sun, X. *Angew. Chem., Int. Ed.* **2011**, *50*, 422–426.
(5) Koenigsmann, C.; Santulli, A. C.; Gong, K.; Vukmirovic, M. B.; Zhou, W.-P.; Sutter, E.; Wong, S. S.; Adzic, R. R. *J. Am. Chem. Soc.* **2011**, *133*, 9783–9795.
(6) Yang, S.; Hong, F.; Wang, L.; Guo, S.; Song, X.; Ding, B.; Yang, Z. *J. Phys. Chem. C* **2010**, *114*, 203–207.
(7) (a) Chen, M.; Kim, J.; Liu, J. P.; Fan, H.; Sun, S. *J. Am. Chem. Soc.* **2006**, *128*, 7132–7133. (b) Metin, O.; Mazumder, V.; Ozkar, S.; Sun, S. *J. Am. Chem. Soc.* **2010**, *132*, 1468–1469.

(8) Lu, X.; Au, L.; McLellan, J.; Li, Z.-Y.; Marquez, M.; Xia, Y. *Nano Lett.* **2007**, *7*, 1764–1769.
(9) (a) Wang, C.; Daimon, H.; Onodera, T.; Koda, T.; Sun, S. *Angew. Chem., Int. Ed.* **2008**, *47*, 3588–3591. (b) Wang, C.; Daimon, H.; Sun, S. *Nano Lett.* **2009**, *9*, 1493–1496.
(10) Mazumder, V.; Sun, S. *J. Am. Chem. Soc.* **2009**, *131*, 4588–4589.
(11) Liu, Y.; Chi, M.; Mazumder, V.; More, K. L.; Soled, S.; Henao, J. D.; Sun, S. *Chem. Mater.* **2011**in press(DOI: 10.1021/cm2014785).
(12) Guo, S.; Dong, S.; Wang, E. *Adv. Mater.* **2010**, *22*, 1269–1272.
(13) (a) Chen, Z.; Waje, M.; Li, W.; Yan, Y. *Angew. Chem., Int. Ed.* **2007**, *46*, 4060–4063. (b) Guo, S.; Dong, S.; Wang, E. *Energy Environ. Sci.* **2010**, *3*, 1307–1310.